Sulfuric Activated Carbon of Black Cumin (*Nigella sativa* L.) Seeds for the Removal of Cadmium(II) and Methylene Blue Dye

Patience Mapule Thabede[*], Ntaote David Shooto[*], Thokozani Xaba and Eliazer Bobby Naidoo

Applied Chemistry and Nano-Science Laboratory, Department of Chemistry, Vaal University of Technology, P.O. Box X021, Vanderbijlpark 1900, South Africa

*Corresponding authors: E-mail: mapulepseabelo@gmail.com, ntaotes@vut.ac.za

Carbon from black cumin seeds was modified with 10 and 20% sulfuric acid to obtain the activated adsorbents. Pristine carbon from black cumin seeds, 10 and 20% H_2SO_4 activated carbon from black cumin seeds were labelled CBC, ACBC-10 and ACBC-20, respectively. The adsorbents were characterized by SEM, XRD, FTIR, TGA and BET. The adsorbents maximum trend for Cd(II) was ACBC-10 > ACBC-20 > CBC. The maximum capacity trend for methylene blue dye was ACBC-20 > ACBC-10 > CBC. The kinetic model best fitted pseudo second order for Cd(II) which gave r^2 values of 0.991-0.998. The methylene blue fitted pseudo first order model with r^2 values ranging from 0.993-0.997. Pseudo first order suggested that the adsorption mechanism for methylene blue onto adsorbents involved van der Waal forces of attraction. The equilibrium data fitted Langmuir isotherm model for CBC, ACBC-10 and ACBC-20 with r^2 of 0.994 to 0.998 for the removal of methylene blue whilst the removal of Cd(II) followed Freundlich with r^2 ranging from 0.992 to 0.997. This suggested that the different adsorption processes were involved between the adsorbate and the adsorbents. Gibb′s free energy ($\Delta G°$) for Cd(II) and methylene blue onto CBC, ACBC-10 and ACBC-20 suggested that the reaction was spontaneous. The adsorption of Cd(II) and methylene blue was endothermic, positive values ($\Delta H°$). This suggested that the enthalpy ($\Delta H°$) had a weak interactive force process whose low energy is associated with electrostatic attraction.

Keywords: Activated carbon, Black cumin seeds, Methylene blue, Cadmium(II), Adsorption, sulfuric acid.

INTRODUCTION

The presence of organic dyes in streams and rivers create environmental problem [1]. Hence its elimination is very important due to its toxicity and carcinogenicity. About 15% of dyes are found in industrial effluents during operations and manufacturing processes [2]. Many synthetic dyes have been discovered and usually used in pharmaceutical, chemical, leather, food, paper and textile industries and cannot easily be degraded [3]. Excess of dyes leads to the change of aquatic life properties like chemical oxygen demand (COD), biological oxygen demand (BOD), dissolved oxygen (DO), taste, pH, colour and odour, which ultimately can damage aquatic life [4]. Methylene blue, a cationic dye is not only carcinogenic but also pollutes water environment. Methylene blue can cause abdominal disorders, respiratory disease and blindness [5].

Cadmium is found in fruits, seafood, vegetables, rice and meats. Hence, it is important to control it to minimum especi-

ally in aqueous water [6]. The use of cadmium in industries and discarding of waste containing Cd(II) have led to an increase in the residual concentration of cadmium in water, soil, air and food and its exposure is associated with many health effects of acute exposure and chronic conditions [7]. Cadmium(II) is one of the most toxic metals, which has an extensive range of sources including, chemical, nuclear, electroplating and electronic industries [8]. Intake of water containing cadmium is harmful and has the risk of causing chronic diseases, such as gastro-intestinal cancer, kidney damage and liver disease also causes Itai-itai disease, hypertension and bone degradation [9,10]. Due to toxic effects of metal ions and dyes on human health, the removal of these pollutants is compulsory before it adds in the environment and passes into the human food chain.

Reverse osmosis [11,12], chemical precipitation [13], electro-dialysis [14], ion-exchange [15] and many others are conven-tional methods employed for the removal of dyes and metal ions from aqueous solutions. Disadvantages of these

conventional treatment technologies like partial removal of certain ions espe-cially at low concentration and high cost often make these processes not to be ideal. Adsorption process is an alternative method in comparison with the other techniques, it provides many opportunities such efficiency, low cost, easy operation and control, high potential to bring about the separation more effectively [9].

Among the various adsorbents, studies have shown that low cost activated carbon obtained from biomass has a potential for removing toxic metals and dyes due to chemical inter-actions of polar functional groups, such as hydroxyl, carboxylic and amino groups and also due to their high surface area, high degree of porosity, which leads to high adsorption capacity [16]. The use of biomass as a source of carbon has other advantages such as availability, low cost, renewability and ecological suit-ability [17]. In this study, low cost carbonized black cumin seeds were chemically activated using 10 and 20% of sulfuric acid at 200 ºC. The adsorbents were labelled carbonized black cumin (CBC), 10% activated carbon black cumin (ACBC-10) and the 20% activated carbon black cumin (ACBC-20) seeds. The three prepared adsorbents CBC, ACBC-10 and ACBC-20 were used for adsorptive studies of Cd(II) and methylene blue under different experimental parameters such as temperature, concentration and contact time. Sorption properties towards methylene blue dye and Cd(II) of the prepared activated carbon are also discussed.

EXPERIMENTAL

Black cumin seeds were bought from health shop located in Vanderbijlpark, Vaal triangle, South Africa. Cadmium acetate $Cd(CH_3COO)_2$ 99.995%, sulphuric acid 98% A.R grade and methylene blue ($C_{16}H_{18}N3SCl$) 82% were purchased from Sigma-Aldrich South Africa Ltd.

Carbonized black cumin seeds adsorbent: Adsorbents preparation method was adopted from Shooto *et al.* [18]. The untreated black cumin seeds were washed dried and grounded. The grounded black cumin seeds were carbonized at 200 ºC in catalytic vapour deposition (CVD) furnace in nitrogen atmos-phere thereafter they were labelled (CBC).

Activated black cumin (ACBC)-10 adsorbent: The carbonized (200 ºC) black cumin seeds were activated with 10% H_2SO_4 and labelled ACBC-10. The adsorbent was agitated for 24 h then rinsed with distilled water several times and dried in the oven for 24 h. The obtained brownish-black material was used for adsorption studies.

Activated black cumin (ACBC)-20 adsorbent: The carb-onized adsorbent was activated with 20% H_2SO_4 then agitated for 24 h. After elapsed time the adsorbent was rinsed with double distilled water then dried for 24 h. This adsorbent was labelled ACBC-20. The obtained black material was ready for charac-terization.

Concentration effect: Each adsorbents CBC, ACBC-10 and ACBC-20 (0.1 g) were weighed into sample vials. Methylene blue dye (20 mL) with standard solutions of 20, 40, 60, 80 and 100 mg/L was transferred into each vial containing 0.1 g. The solutions and the adsorbents were agitated for 60 min on a shaker. The mixture was centrifuge and decanted. The decanted solutions were used for analysis. The same procedure was used for cadmium(II).

Contact time effect: About 0.1 g of adsorbent was weighed and then transferred into nine vials. Each vial containing the weighed adsorbent was added 20 mL Cd(II) solution with a standard concentration of 100 ppm from $Cd(CH_3COO)_2$ solution. The mixture was agitated on a shaker for each time interval of 1, 5, 10, 15, 20, 30, 60, 90 and 120 min, respectively. The solutions were centrifuge then decanted and stored for analysis. The same method was followed using methylene blue dye.

Temperature effect: Accurately weighed CBC, ACBC-10 and ACBC-20 (0.1 g each) were placed into five test tubes. Methylene blue solution (20 mL) with concentration of 100 ppm was transferred into each vial containing the adsorbents. The effect of temperature was carried out at 25, 30, 40, 60 and 80 ºC. The mixture was put in a water bath for 60 min. The solution with adsorbents were centrifuged and decanted. The decanted solutions were used for analysis. The same procedure was used for the metal ion.

pH effect: Each adsorbent (0.1 g) was weighed then placed into five sample vials. Cadmium acetate (20 mL) solution with a standard concentration of 100 ppm was transferred to each vial containing the weighed adsorbents. The initial pH of each solution was measured and thereafter adjusted with 0.1 M of HNO_3 and 0.1 M NaOH to pH of 1, 3, 5, 7 and 9. The mixtures were agitated on a shaker for 60 min. After 60 min, the mixtures were centrifuged then decanted. The solutions were collected and used for Cd(II) analysis. The same procedure was followed for methylene blue.

Characterization: The chemical features of the adsorbent were determined by scanning electron microscope (SEM), Fourier transform infrared (FTIR), thermogravimetric analysis (TGA) and X-ray diffractometer (XRD). The surface morpho-logy measurements were determined using field emission scanning microscopy (FE-SEM)-ZEISS ultra plus, Germany. Nicolet iS50 FTIR spectrometer 400 was used with measuring range from 4000 to 520 cm^{-1}. TGA 4000 thermogravimetric analyzer, Perkin-Elmer was used at a heating rate of 10 ºC/min under a nitrogen atmosphere between 30-900 ºC. Shimadzu XRD 7000 was used to identify crystalline phase of the samples with scan speed set at 10 º/min and scan range set from 10 to 80º. Hach Precision pH meter was used to measure pH using deionized water and pH at point of zero charge pH_{PZC} was evaluated using the pH drift method. Ultraviolet-visible (UV-Vis) spectrometer spectroscopy Perkin-Elmer Lambda 25 was used for methylene blue dye with the visible range using a slit of 1.0 and width of 0.1.

Data analysis: The adsorbed amount of cadmium(II) and methylene blue onto the adsorbents was determined using the following equation for batch dynamic studies:

$$q_e = \frac{V(C_o - C_e)}{m} \tag{1}$$

where q_e is the Cd(II) and methylene blue concentration sorbed onto the adsorbents at equilibria point (mg of metal ion/g of adsorbent); C_o is the initial concentration of cadmium(II) and methylene blue in solution (ppm); C_e is the equilibria point concentrations of Cd(II) and methylene blue in solution (ppm); V is the initial volume of Cd(II) and methylene blue solutions used (L) and m is the weight of the adsorbents

Eqns 2 and 3 are the non-linear forms which were used to determine the kinetics models; pseudo-first order (PFO) and pseudo-second order (PSO). The amounts of metal ions adsorbed (mg/g) are q_e and q_t at equilibrium and time (t). The k_1 is the rate constant of PFO in min^{-1}; and k_2 is the rate constant of PSO (g mg^{-1} min^{-1}).

$$q_e = q_t(1 - e^{-k_1 t}) \tag{2}$$

$$q_e \frac{1 + k_2 q_e t}{k_2 q_e^2 t} \tag{3}$$

The collected data was integrated into eqn 4 to calculate the intra-particle diffusion (IPD) model. The amounts adsorbed (q_t) and rate constant (k_i) were evaluate using the KyPlot software, (k_i) the rate constant (g g^{-1} $min^{1/2}$) and C is the concentration of metal ions on the adsorbent surface.

$$q_t = k_i(t^{1/2}) + C \tag{4}$$

To calculate the adsorption isotherms for Langmuir and Freundlich respectively eqns 5 and 6 were used. Solute surface interaction energy (b), $(Q_o)_{max}$ is the maximum capacity of the adsorbent (mg/g), Freundlich capacity factor (k_f) and (1/n) is the isotherm linearity parameter.

$$q_e = \frac{Q_0 b C_e}{1 + b C_e} \tag{5}$$

$$q_e = k_f C_e^{1/n} \tag{6}$$

Eqn 7 was used to evaluate the thermodynamic function values; equilibrium constant (K_c).

$$K_C = \frac{q_e}{C_e} \tag{7}$$

Other thermodynamic functions namely; enthalpy (ΔH°), entropy (ΔS°) and Gibbs free energy (ΔG°) were determined using eqns 8 and (9) at 25, 30, 40, 60 and 80 °C.

$$\ln K_C = \frac{\Delta H^\circ}{RT} - \frac{\Delta S^\circ}{R} \tag{8}$$

$$\Delta G^\circ = -RT \ln K_C \tag{9}$$

RESULTS AND DISCUSSION

Characterization of the surface morphology and physical properties of the adsorbents was carried out using SEM. Figs. 1a-f show the surface morphology of CBC, ACBC-10 and ACBC-20. Images of CBC (Figs. 1a-b) show that the adsorbent consist of cavities and tiny pores on the surface which may be taken as a sign that adsorption of Cd(II) and dye molecules can take place in the cavities and pores. A similar trend was observed in Figs. 1c-d and e-f for ACBC-10 and ACBC-20, respectively with shiny smooth surfaces that have small spots.

FTIR analysis: The FTIR spectroscopy was used to tract changes that has occurred after the activation. FTIR spectra of CBC, ACBC-10 and ACBC-20 are shown in Fig. 2 with broad peaks at 3287, 3279 and 3295 cm^{-1}, which were due to (-OH) stretching, respectively. The small peaks at 3008 cm^{-1} were observed in all spectra which were assigned to (-CH). These peaks are due to oil in the samples composition in fatty acids which was observed on the three adsorbents [19]. The two bands of (-CH$_3$) and (-CH$_2$) which was attributed to (-CH) stretch were observed at 2922 and 2853 cm^{-1} on CBC, 2923 and 2853 cm^{-1} on ACBC-10 and 2922 to 2853 cm^{-1} on ACBC-20, respectively. The sharp peak at 1743 cm^{-1} due to ketonic group (-C=O) [20] was observed on all adsorbents. The band at 1651 cm^{-1} on ACBC-10 and ACBC-20 was attributed to the vibration of (C=O) of the carbonyl structure [21], the peak shifted to 1649 cm^{-1} on CBC. The peak at this region might be with (N-H) deformation of amino and amide groups along with C=O stretching vibration of amides [10]. There was a new peak due to (N-H) at 1530
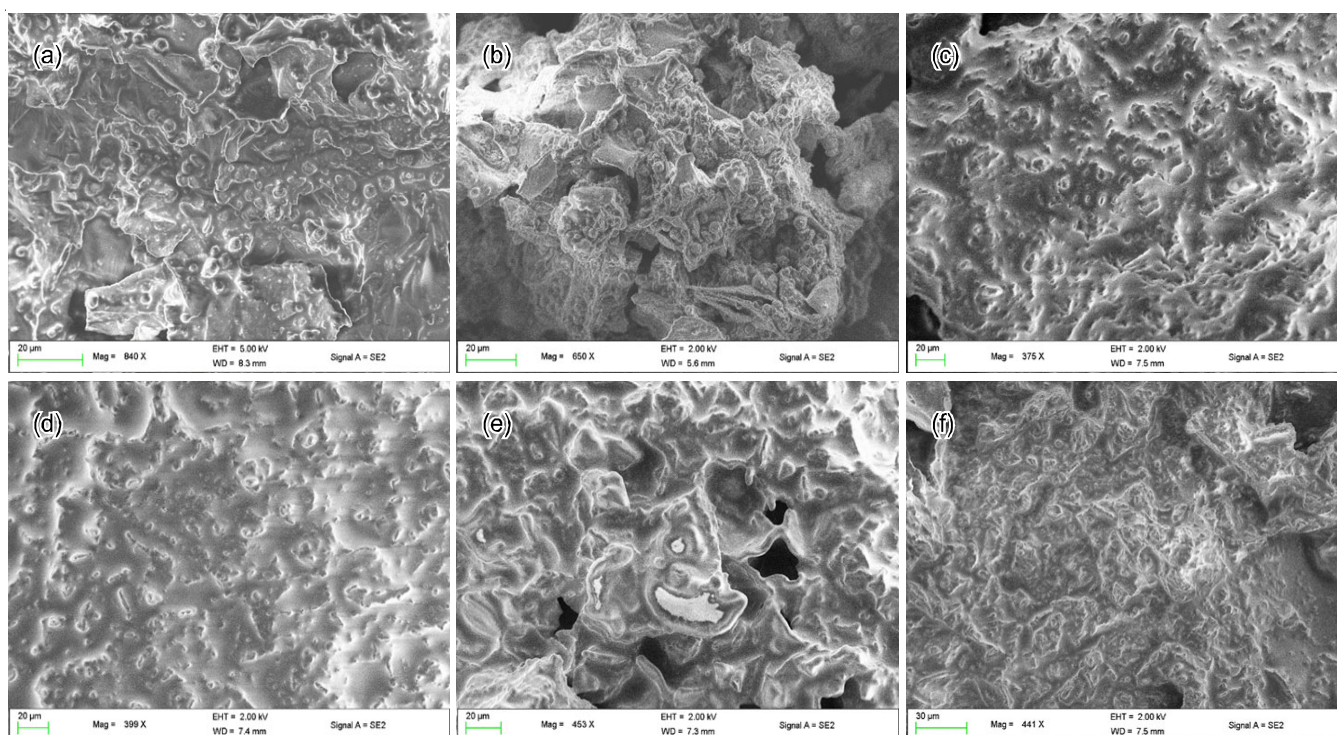

Fig. 1. (a,b) SEM images of CBC. (c,d) ACBC-10. (e,f) ACBC-20 adsorbents
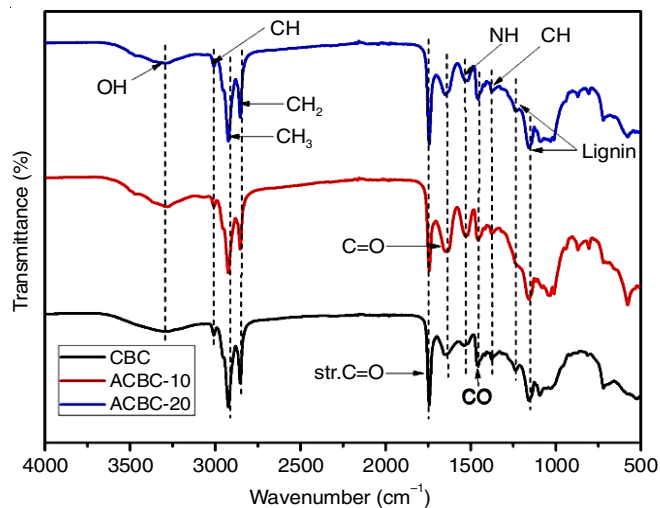
Fig. 2. IR spectra of CBC, ACBC-10 and ACBC-20 adsorbents

Fig. 4. TGA of CBC, ACBC-10 and ACBC-20 adsorbents

cm^{-1} on ACBC-10 which shifted to 1527 cm^{-1} on ACBC-20, then it dropped off on CBC [22]. The peaks at 1457, 1455 and 1456 cm^{-1} were assigned to (-CO) group stretching band of CBC, ACBC-10 and ACBC-20, respectively. The band at 1377 cm^{-1} on CBC, ACBC-10 and ACBC-20 was due to (-CH) and was associated with the deformation of cellulose and hemi-celluloses [23]. The other bands at 1240 and 1157 cm^{-1} on all adsorbents were attributed to structures of hemicellulose and cellulose and lignin [24].

XRD analysis: The X-ray diffraction patterns of CBC, ACBC-10 and ACBC-20 are shown in Fig. 3. The broad peak at 2θ between 15° and 21° on CBC, ACBC-10 and ACBC-20 is assi-gned to cellulosic content of the adsorbents. CBC shows a tall narrow peak at 2θ (62°) and disappeared on ACBC-10 and ACBC-20. The other peaks were assigned to the amorphous nature of adsorbents.
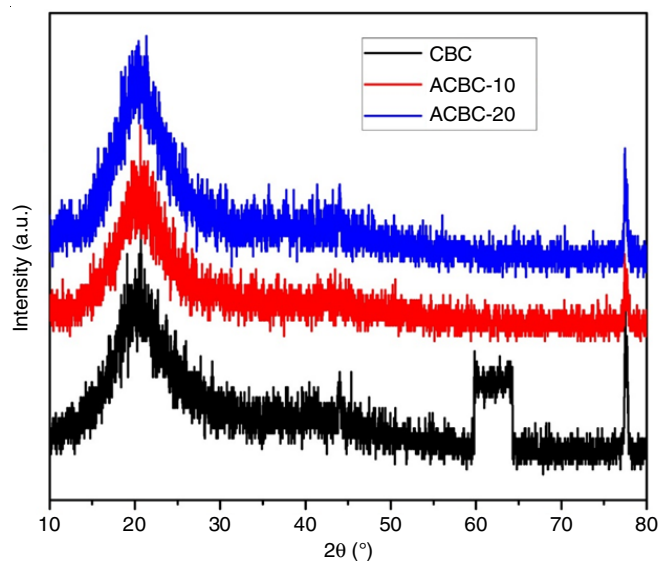

Fig. 3. XRD spectra of CBC, ACBC-10 and ACBC-20 adsorbents

Fig. 4 shows the thermal stability profiles of CBC, ACBC-10 and ACBC-20 conducted in nitrogen atmosphere. The plot showed two main decomposition steps namely, the first stage between 34 and 174 °C due to dehydration of water on the surface
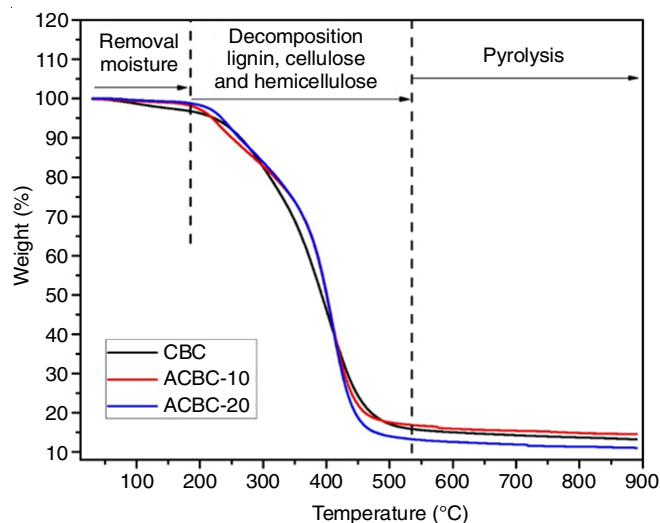
of the adsorbents. Samples weight loss percentages are 4, 2, and 1% for CBC, ACBC-10 and ACBC-20, respectively. The second decomposition between 174 and 516 °C is attributed to the breaking down of lighter volatiles hemicellulose then the heavier cellulose and lignin [25] with weight percentage of 81, 80 and 86% for CBC, ACBC-10 and ACBC-20, respectively. After the degradation of lignocellulose materials, a long tail from 516-900 °C was due to pyrolysis of residues formed during the breaking down of cellulose, hemicellulose and lignin was observed.

Adsorption studies: The effect of adsorption concentration at different concentrations (20, 40, 60 80 and 100 ppm) was studied to determine sorption ability of CBC, ACBC-10 and ACBC-20 at constant temperature of 25 °C for methylene blue and cadmium(II) in aqueous solution is shown in Fig. 5. The adsorption rate was rapid at lower concentrations between 20 and 60 ppm solutions. This might be attributed to the presence of vacant bounding sites and free pore space on the surface of CBC, ACBC-10 and ACBC-20. As the concentration increased the sorption capability started to slow down indicating the saturation of vacant sites and pores [26]. Thereafter, no further increase of capacity was observed which indicated that equilibrium was reached. The maximum capacity of adsorption of methylene blue were 15.11 mg/g on CBC, 15.89 mg/g on ACBC-10 and 16.00 mg/g on ACBC-20 with maximum capacity trend as ACBC-20 > ACBC-10> CBC. Cadmium(II) maximum capacities were; 6.27 mg/g on CBC, 7.61 mg/g on ACBC-10 and 7.14 mg/g ACBC-20. Adsorbents maximum capacity trend for Cd(II) was ACBC-10>ACBC-20 >CBC. It was observed that the adsorbents were selective towards pollutants. Table-1 shows isotherm parameters of CBC, ACBC-10 and ACBC-20, which were evaluated at 25 °C in order to determine inter-action behaviour and capacity of the adsorbents. The sorption of methylene blue on all adsorbents followed Langmuir iso-therm model with r^2 between 0.994-0.998 whilst cadmium(II) fitted Freundlich isotherm model with r^2 between 0.992-0.997, which was close to the unity. The Langmuir isotherm model indicates that the adsorption took place on active sites and has equal attraction for adsorbates and also implies that there is monolayer adsorption occurring on dye surface. The Freundlich
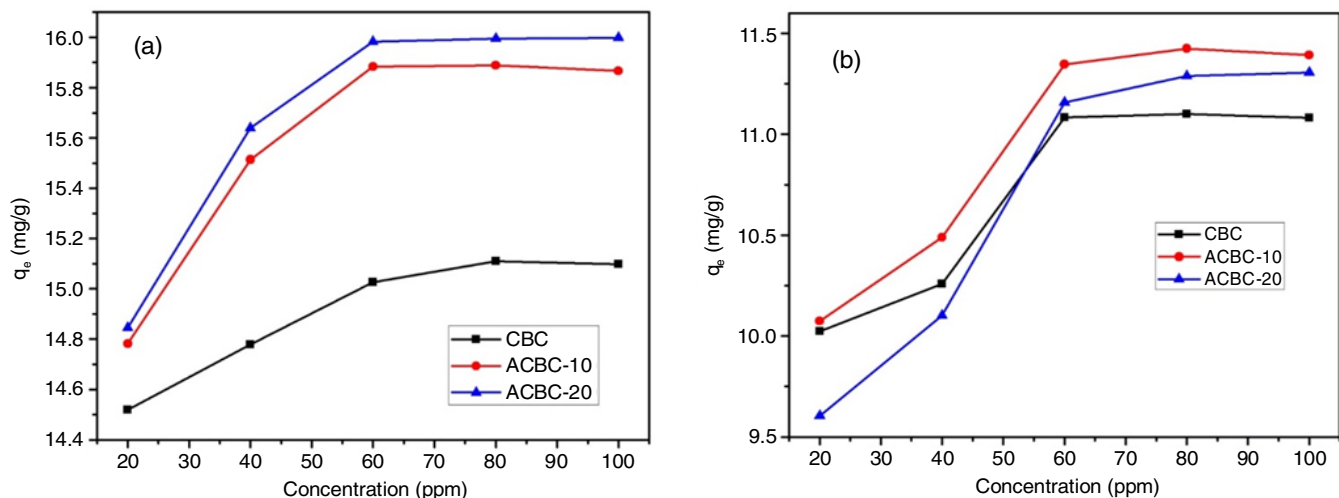
Fig. 5. Concentration effect of methylene blue-(a) and Cd(II)-(b) onto CBC, ACBC-10 and ACBC-20 adsorbents

		CBC		ACBC-10		ACBC-20	
TABLE-1 ISOTHERMS STUDIES AND THEIR PARAMETERS							
Isotherms		Cd(II)	Methylene blue	Cd(II)	Methylene blue	Cd(II)	Methylene blue
Langmuir	Q_o	13.34	15.47	15.68	23.03	13.16	21.54
	B	0.24	0.857	0.27	0.15	0.16	0.51
	r^2	0.902	0.998	0.904	0.994	0.914	0.997
Freundlich	$1/n$	53.34	25.67	45.68	23.03	46.15	21.54
	k_f	5.10	0.56	0.22	0.43	1.14	0.75
	r^2	0.992	0.821	0.995	0.903	0.997	0.911
Experimental	q_e	11.09	15.11	11.31	16.00	11.36	16.01

model suggest that the process involves multi-layer adsorption with interactions between the adsorbate and the adsorbent, it further proposed that surface was heterogeneous in nature.

The rate at which cadmium(II) and methylene blue was removed from aqueous solution was important, hence, we had to evaluate and determine the efficiency of CBC, ACBC-10, ACBC-20 for wastewater treatment. The efficiency of CBC, ACBC-10, ACBC-20 were determined using the time intervals of 5, 10, 15, 20, 30, 40, 60, 90 and 120 min as indicated in Fig. 6. The plots show that sorption was rapid within the first

30 min, this is because of unoccupied active sites at the initial stage of the sorption process. However, as the time increased the sorption sites decreased in number and got saturated. The maximum capacities were 13.19 mg/g on CBC, 15.25 mg/g on ACBC-10 and 16.42 mg/g on ACBC-20 for methylene blue and 12.01 mg/g on CBC, 13.66 mg/g on ACBC-10 and 12.57 mg/g on ACBC-20 for Cd(II). To calculate the kinetic parameters, three kinetic models were used and kinetic data is shown in Table-2 for methylene blue and Cd(II) onto CBC, ACBC-10 and ACBC-20. The three models were pseudo first order
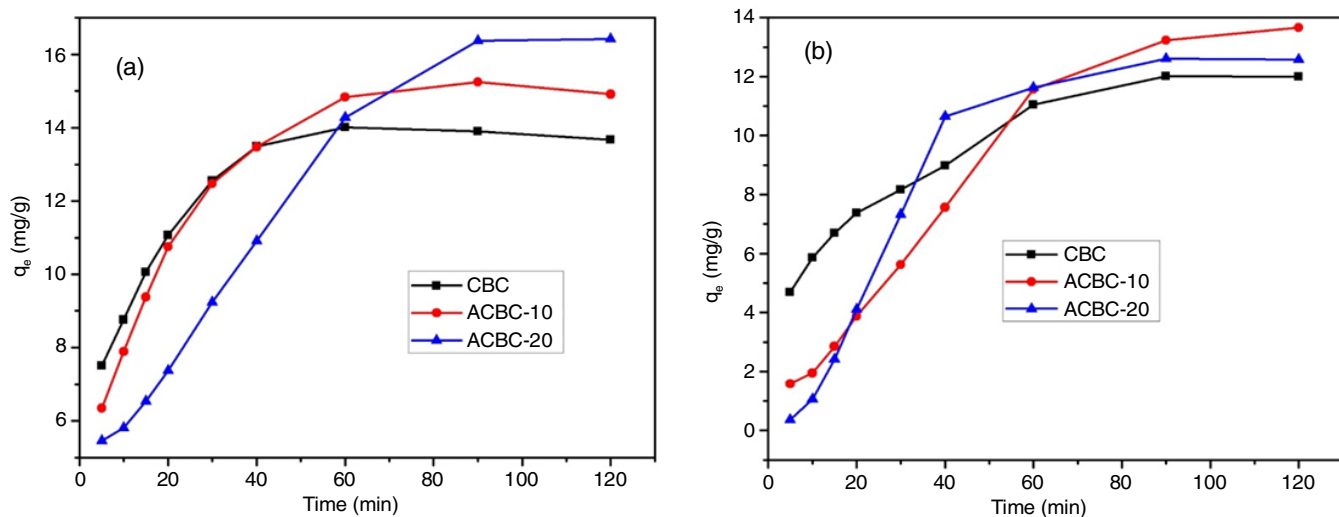

Fig. 6. Time effect of methylene blue-(a) and Cd(II)-(b) onto CBC (filled square), ACBC-10 (filled circle) and ACBC-20 (filled triangle) adsorbents

Models		CBC		ACBC-10		ACBC-20	
		Cd(II)	Methylene blue	Cd(II)	Methylene blue	Cd(II)	Methylene blue
PFO	q_e	13.07	14.66	14.05	14.72	12.16	17.66
	K_1	4.09	4.07	4.19	0.073	4.23	4.13
	r^2	0.808	0.993	0.877	0.997	0.838	0.996
PSO	q_e	9.87	4.83	8.44	8.14	6.08	4.08
	K_2	0.023	0.056	0.020	0.085	0.022	0.030
	r^2	0.998	0.872	0.991	0.895	0.993	0.874
IPD	C	4.177	5.097	3.515	4.556	7.54	5.39
	K_i	6.81	5.34	7.716	1.79	1.89	1.35
	r^2	0.933	0.715	0.909	0.769	0.976	0.759
EPA[a]	%	83.60	71.28	72.47	71.69	66.55	69.21
ESA[a]	%	16.40	28.72	27.52	28.31	33.45	30.79
Experimental	(q_e)	13.37	14.01	13.23	15.24	12.57	16.42

TABLE-2
KINETIC MODELS AND THEIR PARAMETERS

[a]EPA = Estimated pore adsorption of IPD and *ESA = Estimated surface adsorption of IPD.

(PFO), pseudo second order (PSO) and intraparticle diffusion (IPD) models. In order to evaluate whether the adsorption has a good fit for the PFO or PSO, the values of correlation coefficient must be close to 1 and the values of adsorption capacity need to be close to the experimental data. The data showed that the adsorption of methylene blue on all adsorbents best fitted PFO model with r^2 values ranging from 0.993-0.997 whilst Cd(II) data fitted PSO with r^2 values of 0.991-0.998. The adsorption mechanism of PFO propose that Cd(II) on the adsorbents involved van der Waal forces attraction and PSO indicates that the adsorption process on methylene blue was dependent on the availability of the adsorption sites. The nature of the process was estimated using IPD kinetic model which evaluates whether adsorption takes place on the surface (ESA) or pores (EPA). The estimated pore adsorption (EPA) was observed in all adsorbents.

Effect of temperature: A sequence of experiments were accomplished at different temperatures to investigate the effect of temperature to the sorption of methylene blue and Cd(II) dyes on CBC, ACBC-10 and ACBC-20. The effect of temperature was determined at 25, 30, 40, 60 and 80 °C as shown in Fig. 7. The plots showed that there is an increase in adsorption capacities as the temperature from 25 to 60 °C in Fig. 7a for

methylene blue. As the temperature increased further from 60 to 80 °C resulted in reduced adsorption capacities and hence reaching equilibrium. This suggests at high temperatures there is more kinetic energy which makes molecules to move fast in the solution which in turn decrease interaction with the active sites for adsorption to occur. Fig. 7b shows slight different patterns in that as the temperature increases the capacity increased as well. This suggested that the adsorption of Cd(II) in this study prefer a slight increase in temperature in order to improve the adsorption process. The thermodynamic parameters *viz.* enthalpy ($\Delta H°$), Gibbs free energy ($\Delta G°$) and entropy ($\Delta S°$) are shown in Table-3. The $\Delta G°$ for all CBC, ACBC-10 and ACBC-20 were negative indicated that the reaction was exothermic and spontaneous and $\Delta H°$ as well as $\Delta S°$ were positive. The positive value of $\Delta H°$ indicates that Cd(II) biosorption is an endothermic process [27], which in turn explains the temperature enhanced Cd(II) biosorption as shown in Fig. 7b.

Effect of pH: The effect of pH was studied at pH 1, 3, 5, 7 and 9 for methylene blue and Cd(II) on CBC, ACBC-10, ACBC-20. The adsorption capacity of methylene blue and Cd(II) was largely dependent of pH. The adsorption of methylene blue (Fig. 8a) was steadily increased with increasing pH 1 to
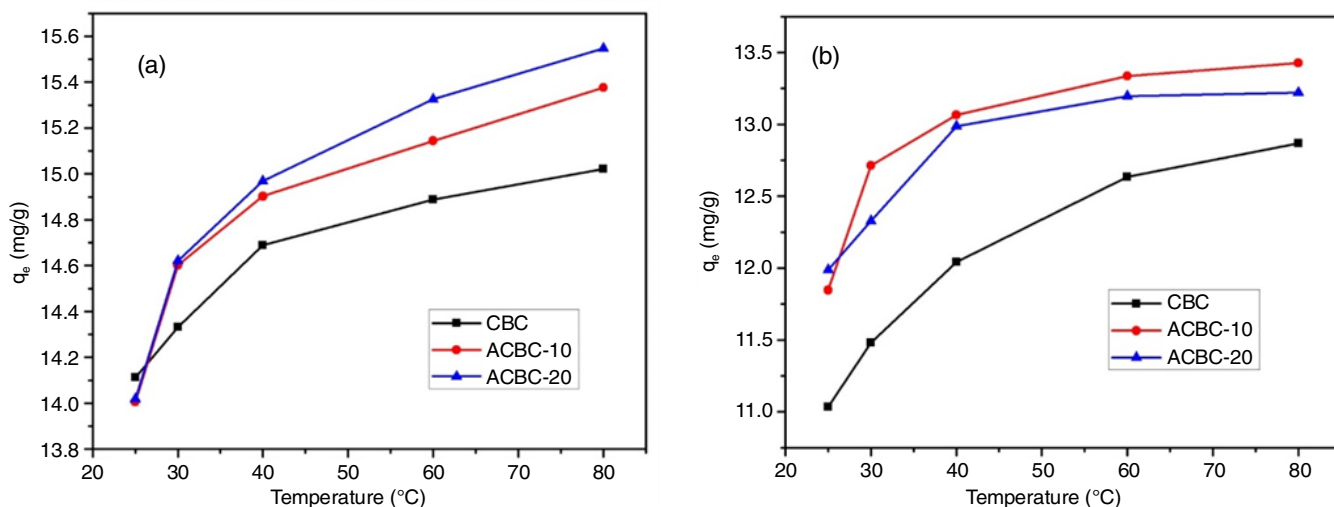

Fig. 7. Temperature effect of methylene blue-(a) and Cd(II)-(b) onto CBC (filled square), ACBC-10 (filled circle) and ACBC-20 (filled triangle) adsorbents

| | TABLE-3 | | | | | |
| | THERMODYNAMIC STUDIES AND THEIR PARAMETERS | | | | | |
| Parameter | CBC | | ACBC-10 | | ACBC-20 | |
	Cd(II)	Methylene blue	Cd(II)	Methylene blue	Cd(II)	Methylene blue
$\Delta H°$ (KJ mol^{-1})	1.3×10^{-3}	2.1×10^{-2}	1.4×10^{-3}	1.5×10^{-3}	1.3×10^{-3}	9.0×10^{-4}
$\Delta S°$ (KJ mol^{-1}K^{-1})	1.6×10^{-3}	1.8×10^{-3}	1.6×10^{-3}	2.3×10^{-3}	1.8×10^{-3}	2.7×10^{-3}
$\Delta G°$ (KJ mol^{-1}) 298 K	-3.47	-1.82	-3.06	-1.88	-2.99	-1.87
303 K	-3.30	-1.72	-2.65	-1.55	-2.86	-1.72
313 K	-3.11	-1.54	-2.54	-1.40	-2.84	-3.39
333 K	-2.96	-1.49	-2.53	-1.31	-2.95	-0.85
353 K	-2.89	-1.48	-2.42	-1.21	-2.90	-0.61
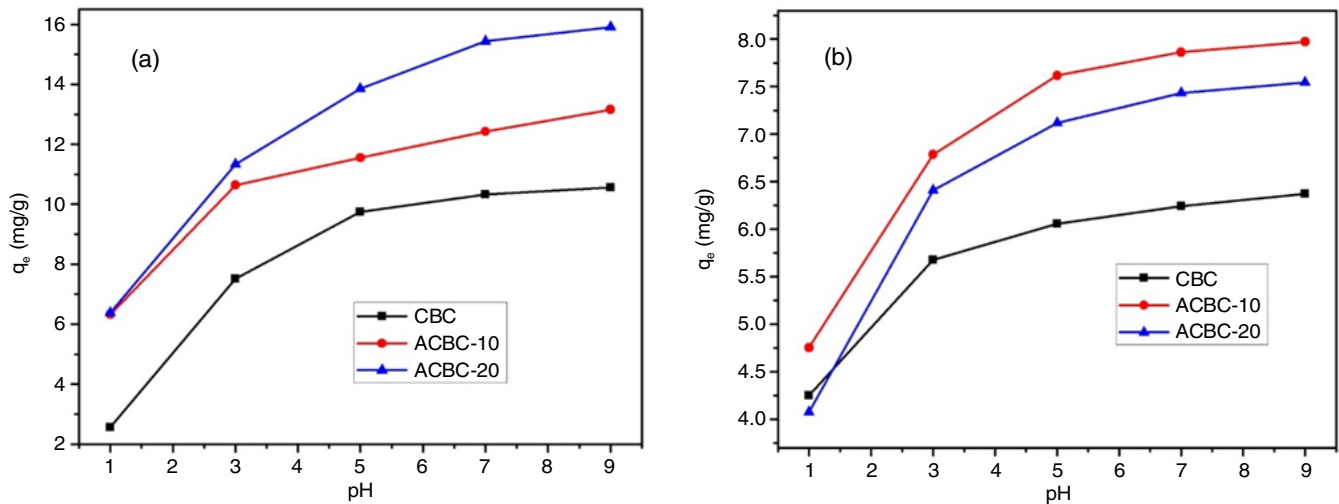
Fig. 8. pH effect of methylene blue-(a) and Cd(II)-(b) onto CBC (filled square), ACBC-10 (filled circle) and ACBC-20 (filled triangle) adsorbents

5. A similar trend was observed for Cd(II). This suggests that at low pH the solution is protonated due to functional groups (-COOH, -OH and -NH$_2$) on the adsorbent surface hence low adsorption due to repulsion force. At higher pH 7-9, there was less repulsion force between the adsorbent surface and the functional groups due to deprotonation hence an increase in adsorption capacity [18]. The increase in negative charges of the adsorbent surface benefits, improved the forces of attraction and the adsorption capacity.

Point of zero charge is an important characteristic which evaluates the point at which the adsorbent surface has net electrical neutrality [17]. Fig. 9 shows the plots of ΔpH vs. pH$_i$ of CBC, ACBC-10 and ACBC-20. The point of zero charge attained was 5.7 on CBC and 2.3 for both ACBC-10 and ACBC-20. The pH$_i$-pH$_f$ values were negative before 2.3 and 5.7. This indicates that the pH$_{pzc}$ is less than pH 7.00, causing an increase in the negative charge density on the surface of activated carbon for adsorption of methylene blue and Cd(II). The pH values above pH$_{PZC}$ 2.3 and 5.7 showed that CBC, ACBC-10, ACBC-20 surfaces acquired positive charge and ΔpH values became positive.

Comparative studies: Table-4 shows different adsorbents used for the removal of Cd(II) and methylene blue dye from aqueous solutions. From the data, it is cle ar that activated black cumin seeds can be used for adsorption of Cd(II) and methylene blue dye. Activated black cumin seeds (CBC, ACBC-10 and ACBC-20) adsorption studies showed a
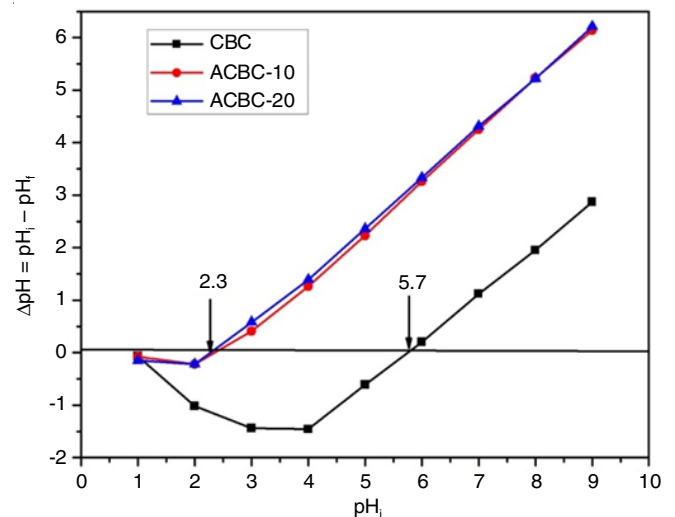

Fig. 9. Point zero charge of methylene blue and Cd(II) onto CBC (filled square), ACBC-10 (filled circle) and ACBC-20 (filled triangle) adsorbents

potential and good removal capacity in comparison to some of the previously reported biosorbents.

Conclusion

In this work, a low cost black cumin seeds were carbonized and activated with 10 and 20% H$_2$SO$_4$ for the adsorption of methylene blue dye and cadmium(II) ions. Adsorption process was evaluated using different parameters such as time, concen-

TABLE-4
COMPARISON OF Cd(II) AND METHYLENE BLUE ADSORPTION CAPACITY WITH OTHER ADSORBENTS

Cd(II)			Methylene blue		
Adsorbents	$q_{(max)}$ (mg/g)	Ref.	Adsorbents	$q_{(max)}$ (mg/g)	Ref.
Corn stalks	41.17	[28]	Lignin-chitosan	36.25	[37]
Graphene oxide	23.9	[29]	Fly ash	30.1	[38]
H. valentiae	17.0	[30]	Palm oil	22.4	[39]
Black cumin seeds	13.66	This study	Black cumin seeds	16.42	This study
Sugar cane bagasse	14.8	[31]	Coconut shell	15.1	[40]
Cocoa pod husk biomass	13.4	[32]	Palygorskite clay	14.0	[41]
Acrylonitrile modified corn stalk	12.7	[33]	Fly ash	9.8	[42]
Buffalo weed	11.6	[34]	Sugar spent rice biomass	8.1	[43]
Chicken feathers	7.8	[35]	Yellow passion fruit shell	6.8	[44]
Alhaji maurorum seed	3.7	[36]	*Caulerpa racemose* var. cylindracea	5.2	[45]

tration and pH. The results showed that maximum capacity trend for Cd(II) was in order of ACBC-10 > ACBC-20 > CBC and for methylene blue ACBC-20 > ACBC-10 > CBC. Adsorption kinetics of CBC, ACBC-10 and ACBC-20 both Cd(II) ions and methylene blue was fast. The data showed that the adsorption of methylene blue on all adsorbents best fitted pseudo first order (PFO) whilst Cd(II) data fitted pseudo second order (PSO) model. Isotherms best fitted Freundlich model for Cd(II), while methylene blue fitted Langmiur model for methylene blue. The entropy ($\Delta S°$) was positive which indicated the randomness and degree of freedom for methylene blue and Cd(II) in the solution during sorption process whilst ($\Delta G°$) with negative values suggested that the sorption processes for CBC, ACBC-10 and ACBC-20 was spontaneous. This work affirms the use of black cumin seeds as adsorbents for the adsorption of methylene blue dye and Cd(II) from aqueous solution.

CONFLICT OF INTEREST

The authors declare that there is no conflict of interests regarding the publication of this article.

REFERENCES

1. A.B. Albadarin, M.N. Collins, M. Naushad, S. Shirazian, G. Walker and C. Mangwandi, *Chem. Eng. J.*, **307**, 264 (2017);
    https://doi.org/10.1016/j.cej.2016.08.089
2. D. Pathania, S. Sharma and P. Singh, *Arab. J. Chem.*, **10**, S1445 (2017);
    https://doi.org/10.1016/j.arabjc.2013.04.021
3. Ravi and L.M. Pandey, *Appl. Clay Sci.*, **169**, 102 (2019);
    https://doi.org/10.1016/j.clay.2018.12.019
4. B. Lellis, C.Z. Fávaro-Polonio, J.A. Pamphile and J.C. Polonio, *Biotechnol. Res. Innov.*, **3**, 275 (2019);
    https://doi.org/10.1016/j.biori.2019.09.001
5. R.M. Novais, G. Ascensao, D.M. Tobaldi, M.P. Seabra and J.A. Labrincha, *J. Clean. Prod.*, **171**, 783 (2018);
    https://doi.org/10.1016/j.jclepro.2017.10.078
6. N. Kawasaki, H. Tominaga, F. Ogata and K. Kakehi, *Chem. Eng. J.*, **157**, 249 (2010);
    https://doi.org/10.1016/j.cej.2009.11.028
7. A.A. Al-Homaidan, J.A. Alabdullatif, A.A. Al-Hazzani, A. Al-Ghanayem and A.F. Alabbad, *Saudi J. Biol. Sci.*, **22**, 795 (2015);
    https://doi.org/10.1016/j.sjbs.2015.06.010
8. Y. Zhang, Q. He, L. Xia, Y. Li and S. Song, *Biochem. Eng. J.*, **138**, 179 (2018);
    https://doi.org/10.1016/j.bej.2018.07.021
9. H. Sharififard, Z.H. Shahraki, E. Rezvanpanah and S.H. Rad, *Bioresour. Technol.*, **270**, 562 (2018);
    https://doi.org/10.1016/j.biortech.2018.09.094
10. M. Basu, A.K. Guha and L. Ray, *Process Saf. Environ.*, **106**, 11 (2017);
    https://doi.org/10.1016/j.psep.2016.11.025
11. L. Lin, X. Xu, C. Papelis, T.Y. Cath and P. Xu, *Sep. Purif. Technol.*, **134**, 37 (2014);
    https://doi.org/10.1016/j.seppur.2014.07.008
12. B.S. Thaci and S.T. Gashi, *Pol. J. Environ. Stud.*, **28**, 337 (2018);
    https://doi.org/10.15244/pjoes/81268
13. L.K. Wang, D.A. Vaccari, Y. Li and N.K. Shammas, eds.: L.K. Wang, Y.T. Hung and N.K. Shammas, Chemical Precipitation, In: Physicochemical Treatment Processes, Humana Press, New Jersey, vol. 3, pp. 141-198 (2004).
14. F.-M. Allioux, P. Kapruwan, N. Milne, L. Kong, J. Fattaccioli, Y. Chen and L.F. Dumée, *Sep. Purif. Technol.*, **194**, 26 (2018);
    https://doi.org/10.1016/j.seppur.2017.10.064
15. C. Zhao, R. Ge, Y. Zhen, Y. Wang, Z. Li, Y. Shi and X. Chen, *Chem. Eng. J.*, **378**, 122136 (2019);
    https://doi.org/10.1016/j.cej.2019.122136
16. A. Aghababaei, M.C. Ncibi and M. Sillanpaa, *Bioresour. Technol.*, **239**, 28 (2017);
    https://doi.org/10.1016/j.biortech.2017.04.119
17. A. Zubrik, M. Matik, S. Hredzak, M. Lovas, Z. Dankova, M. Kovacova and J. Briancin, *J. Clean. Prod.*, **143**, 643 (2017);
    https://doi.org/10.1016/j.jclepro.2016.12.061
18. N.D. Shooto, P.M. Thabede and E.B. Naidoo, *S. Afr. J. Chem. Eng.*, **30**, 15 (2019);
    https://doi.org/10.1016/j.sajce.2019.07.002
19. M.A. Poiana, E. Alexa, M.F. Munteanu, R. Gligor, D. Moigradean and C. Mateescu, *Open Chem.*, **13**, 689 (2015);
    https://doi.org/10.1515/chem-2015-0110
20. N. Zhou, Y. Wang, D. Yao, S. Li, J. Tang, D. Shen, X. Zhu, L. Huang, M. Zhong and Z. Zhou, *J. Clean. Prod.*, **221**, 63 (2019);
    https://doi.org/10.1016/j.jclepro.2019.02.176
21. M. Barsainya, P. Chandra and D.P. Singh, *Int. J. Curr. Microbiol. Appl. Sci.*, **5**, 274 (2016);
    https://doi.org/10.20546/ijcmas.2016.501.027
22. X. Li, Y. Wei, J. Xu, N. Xu and Y. He, *Biotechnol. Biofuels*, **11**, 263 (2018);
    https://doi.org/10.1186/s13068-018-1251-4
23. T.T.S. Matos, J. Schultz, M.Y. Khan, E.F. Zanoelo, A.S. Mangrich, B.R. Araujo, S. Navickiene and L.P.C. Romao, *J. Braz. Chem. Soc.*, **28**, 1975 (2017);
    https://doi.org/10.21577/0103-5053.20170042
24. M. Husseien, A.A. Amer, A. El-Maghraby and N. Hamedallah, *J. Anal. Appl. Pyrolysis*, **86**, 360 (2009);
    https://doi.org/10.1016/j.jaap.2009.08.003
25. N.D. Shooto, C.W. Dikio, D. Wankasi, L.M. Sikhwivhilu, F.M. Mtunzi and E.D. Dikio, *Nanoscale Res. Lett.*, **11**, 414 (2016);
    https://doi.org/10.1186/s11671-016-1631-2
26. Y. Liu and H. Xu, *Biochem. Eng. J.*, **35**, 174 (2007);
    https://doi.org/10.1016/j.bej.2007.01.020

27. B. Mudyawabikwa, H.H. Mungondori, L. Tichagwa and D.M. Katwire, *Water Sci. Technol.*, **75**, 2390 (2017); https://doi.org/10.2166/wst.2017.041

28. L. Zheng, D. Peng and P. Meng, *J. Clean. Prod.*, **201**, 609 (2018); https://doi.org/10.1016/j.jclepro.2018.08.070

29. Y. Bian, Z.-Y. Bian, J.-X. Zhang, A.-Z. Ding, S.-L. Liu and H. Wang, *Appl. Surf. Sci.*, **329**, 269 (2015); https://doi.org/10.1016/j.apsusc.2014.12.090

30. A. Rathinam, B. Maharshi, S.K. Janardhanan, R.R. Jonnalagadda and B.U. Nair, *Bioresour. Technol.*, **101**, 1466 (2010); https://doi.org/10.1016/j.biortech.2009.08.008

31. U. Garg, M.P. Kaur, G.K. Jawa, D. Sud and V.K. Garg, *J. Hazard. Mater.*, **154**, 1149 (2008); https://doi.org/10.1016/j.jhazmat.2007.11.040

32. V.O. Njoku, A.A. Ayuk, E.E. Oguzie and E.N. Ejike, *Sep. Sci. Technol.*, **47**, 753 (2012); https://doi.org/10.1080/01496395.2011.626829

33. L. Zheng, Z. Dang, X. Yi and H. Zhang, *J. Hazard. Mater.*, **176**, 650 (2010); https://doi.org/10.1016/j.jhazmat.2009.11.081

34. K. Yakkala, M.R. Yu, H. Roh, J.K. Yang and Y.Y. Chang, *Desalination Water Treat.*, **51**, 7732 (2013); https://doi.org/10.1080/19443994.2013.792546

35. W. Yin, C. Zhao, C. Xu, J. Zhang, Z. Guo and Y. Shao, *Colloid Surf. A*, **560**, 426 (2019); https://doi.org/10.1016/j.colsurfa.2018.10.031

36. A. Ebrahimi, M. Ehteshami and B. Dahrazma, *Process Saf. Environ.*, **98**, 374 (2015); https://doi.org/10.1016/j.psep.2015.09.013

37. A.B. Albadarin, M.N. Collins, M. Naushad, S. Shirazian, G. Walker and C. Mangwandi, *Chem. Eng. J.*, **307**, 264 (2017); https://doi.org/10.1016/j.cej.2016.08.089

38. R.M. Novais, J. Carvalheiras, D.M. Tobaldi, M.P. Seabra, R.C. Pullar and J.A. Labrincha, *J. Clean. Prod.*, **207**, 350 (2019); https://doi.org/10.1016/j.jclepro.2018.09.265

39. M.A.A. Zaini, M. Zakaria, S.H. Mohd.-Setapar and M.A. Che-Yunus, *J. Environ. Chem. Eng.*, **1**, 1091 (2013); https://doi.org/10.1016/j.jece.2013.08.026

40. A.M. Aljeboree, A.N. Alshirifi and A.F. Alkaim, *Arab. J. Chem.*, **10**, S3381 (2017); https://doi.org/10.1016/j.arabjc.2014.01.020

41. A. Al-Futaisi, J. Jamrah and R. Al-Hanai, *Desalination*, **214**, 327 (2007); https://doi.org/10.1016/j.desal.2006.10.024

42. V. Basavarao and S. Rammohanrao, *Chem. Eng. J.*, **116**, 77 (2006); https://doi.org/10.1016/j.cej.2005.09.029

43. M.S.U. Rehman, I. Kim and J.-I. Han, *Carbohydr. Polym.*, **90**, 1314 (2012); https://doi.org/10.1016/j.carbpol.2012.06.078

44. F.A. Pavan, A.C. Mazzocato and Y. Gushikem, *Bioresour. Technol.*, **99**, 3162 (2008); https://doi.org/10.1016/j.biortech.2007.05.067

45. S. Cengiz and L. Cavas, *Bioresour. Technol.*, **99**, 2357 (2008); https://doi.org/10.1016/j.biortech.2007.05.011